Journal of Thermal Analysis and Calorimetry, Vol. 95 (2009) 1, 305–312

POLY(3-HYDROXYBUTYRATE-CO-11 MASS%3-HYDROXYVALEATE) MOLDED PART DURING THE SOLIDIFICATION STEP
Temperature and crystallinity profiles

P. M. Stefani, R. A. Ruseckaite and A. Vázquez*

Research Institute of Material Science and Technology, INTEMA-CONICET, Mar del Plata University, Juan B. Justo 4302, 7600 Mar del Plata, Argentina

The numerical simulation of the temperature and relative crystallinity developed across the thickness of a poly(3-hydroxybutyrate-co-11 mass%3-hydroxyvaleate) (PHBV) part upon cooling from the melt as a function of the temperature of the cooling fluid (water) is presented. A modified form of the Avrami equation was used to predict the crystallinity as a function of the temperature. A simple expression was used to relate the kinetic constant k with the temperatures. Temperature profiles were predicted by coupling the above mentioned equations to the one-dimensional unsteady-state thermal energy equation through a heat term describing the crystallization heat. Cooling temperatures were in the range between 20 to 80°C and were restricted by the glass transition temperature of the material and the degree of under-cooling, respectively. Even degrees of crystallinity were predicted for part- thicknesses lower than 10 mm cooled at 60°C, while a fluid temperature of 40°C was more appropriate for a 20 mm – thick part. The model predicted uneven crystallinity profiles for part-thicknesses higher than 30 mm.

Keywords: *biodegradable, crystallization, processing, simulation*

Introduction

Polyhydroxyalkanoates (PHAs), such as poly(3-hydroxybutyrate) (PHB) and its copolymers are naturally occurring thermoplastic polyesters produced by a variety of bacteria as storage intracellular material [1]. These polymers are visualized as potential environmentally friendly substitutes of traditional ones, because their properties are often compared with that of polypropylene [1, 2, 4–6]. The use of PHB in large-scale applications is limited as a consequence of its relatively high cost, thermal instability near the melting point and embrittlement at room temperature attributed to progressive crystallization during storage [7]. One strategy to overcome the drawbacks of PHB is to biosynthesize copolymers containing variable amounts of 3-hydroxyvalerate (3-HV) [1]. Varying the amount of the co-monomer in the copolymer afford co-polyesters with a wide range of melting points and crystallinity with modulated mechanical properties [8]. The presence of 3-hydroxyvalerate units does not affect the thermal stability but seems to act as defects leading a reduction in melting point and crystallization rate [6]. This last observation is critical for processing because during processing operations crystallization is the main phase transition. Indeed, final properties of the part depend on the crystallinity extent, which in turn, depends on the processing conditions.

The crystallization on rapid cooling in a mould of these polymers is subsequently followed by secondary crystallization on storage at room temperature which leads to embrittlement as the crystallinity increases [6, 9, 10]. The crystallization of these polymers at higher temperatures may lead to a better crystalline structure with improved mechanical performance [9].

The understanding of polymer solidification has become nowadays a necessary step in order to predict the final polymer properties. At the present PHB and copolymers with 3-hydroxyvalerate are the only members of PHAs that are commercially available [1]. The cooling stage represents a substantial part of the overall cycle and has a profound effect on the microstructure development and on the ultimate properties of the molded article. Therefore, the development of commercial applications based on these materials requires knowledge of the crystallization behavior under processing conditions. In this sense mathematical simulation can be used to analyze the crystallinity distribution developed upon cooling conditions comparable with the ones normally experienced during industrial processing methods [11–14]. In general, simulation involves solving standard transport equations with appropriate initial and boundary conditions coupled to the crystallization kinetics, in isothermal or non-isothermal conditions [15].

* Author for correspondence: roxana@fi.mdp.edu.ar; ruseckaite@intema.gov.ar

1388–6150/$20.00

Akadémiai Kiadó, Budapest, Hungary
Springer, Dordrecht, The Netherlands

The aim is to predict the microstructure evolution through the thickness of poly(3-hydroxybutyrate-co-11 mass%3-hydroxyvaleate) copolymer (PHBV) molded part developed upon cooling from the melt as a function of the temperature of the cooling fluid (water). A modified form of the Avrami equation was used to predict the crystallinity. The crystallization rate as a function of the temperature was predicted from the experimental calorimetric data previously reported [14]. These equations were coupled to the thermal energy equation through a heat term describing the crystallization heat. The profiles predicted may be helpful in optimizing actual processing conditions.

Non-isothermal kinetic model

Non-isothermal crystallization processes have been traditionally described by integral or differential expressions derived from the classical Avrami equation [16]. Differential expressions are more suitable for modelling purposes and can be easily related to calorimetric data. The integral model of Kamal and Chu [18] is expressed in its differential form by Lin [19] as follow:

$$\frac{\mathrm{d}X_\mathrm{r}}{\mathrm{d}t}=nk(T)(1-X_\mathrm{r})t^{\mathrm{n}-1} \qquad (1)$$

where X_r is the relative crystallinity, n is the Avrami exponent, k is the kinetic constant, T is the temperature and t is the time. This model can be reduced to the classical Avrami expression in isothermal conditions.

The kinetic constant in Eq. (1) depends on the temperature as is described by the following equation [20]:

$$k=k_0\exp\left[\frac{-Ea_2}{R(T-T_\mathrm{g})}\right]\exp\left[\frac{-Ea_1}{R(T_\mathrm{m}^0-T)}\right] \qquad (2)$$

where k_0 is a pre-exponential factor, T_g is the glass transition temperature, T_m^0 is the theoretical melting point, and E_{a_2} and E_{a_1} are the activation energies associated to each exponential. The first exponential accounts for the mobility above T_g, which induces crystallization from the rubbery state (cold crystallization), while the second exponential accounts for the driving force of crystallization given by the degree of undercooling, (T_m^0–T). Kinetic constant takes maximum values between T_g and T_m^0 and crystallization is arrested at these limit temperature values.

The kinetic model can be applied only to crystal growth after nucleation. Nucleation is a thermally activated phenomena and their effect can be detected by isothermal DSC experiment where a signal can be observed only after a delay (induction time) attributed to the formation of nuclei of critical size [20]. The temperature dependence of the induction time (t_i) can be described in isothermal conditions by the following equation [16]:

$$t_\mathrm{i}=k_{\mathrm{i}_0}\exp\left[\frac{E_{\mathrm{i}_2}}{R(T-T_\mathrm{g})}\right]\exp\left[\frac{E_{\mathrm{i}_1}}{R(T_\mathrm{m}^0-T)}\right] \qquad (3)$$

where k_{i_0} is the pre-exponential factor. The two exponential terms are related with the driving force of the nucleation above T_g and below the theoretical melting point; E_{i_1} and E_{i_2} are the activation energies for these contributions. However, the effect of induction time is more complex in non-isothermal crystallization experiments where a time–temperature superposition is verified. The initial condition in a non-isothermal simulation is given by the induction time calculated as the sum of the contributions of several isothermal temperature steps evaluated from the isothermal crystallization experiments. Even if induction time can not be determined experimentally in dynamic conditions, non-isothermal induction time ($t_{\mathrm{n}_\mathrm{i}}$) can be computed by using a dimensionless parameter Q:

$$Q=\int_0^{t_{\mathrm{n}_\mathrm{i}}}\frac{\mathrm{d}t^*}{t_\mathrm{i}} \qquad (4)$$

where t_i is the isothermal induction time given by Eq. (3). Numerical integration of Eq. (4) is performed taking t^*=0 at the melting temperature (T_m^0). The value t^*=$t_{\mathrm{n}_\mathrm{i}}$ at which Q reaches the unity represents the non-isothermal induction time [20, 21].

Physical constants and kinetic parameters used in the simulation are summarized in Table 1. Activation energy (E_i) and pre-exponential factor (k_{0_i}) for the induction time were taken from the literature [22], meanwhile activation energies (E_{a_1} and E_{a_2}) and pre-exponential factor (k_0), were estimated fitting k *vs*. T experimental values (taken from the literature [16]) by using Eq. (2).

Model equations

A thick two-parallel-plates mold was used for the simulation of the solidification process of a macroscopic part made of PHBV and it could be visualized as one-dimensional flow (Fig. 1). This mold is cooled by using water as chilling fluid at a constant temperature.

For modeling purposes, the following assumptions were made:

- The wall of the metallic mold is extremely thin.
- One-dimensional unsteady-state heat transfer rate through the sheet thickness.
- Thermal and physical properties remain constant within the temperature range used in the present study.

Table 1 Physical constant used in the simulation

Physical constant	Values	units	Reference
Thermal conductivity, κ	0.156	J s^{-1} m^{-1} K^{-1}	[22]
Specific heat, C_p	1420	J K^{-1} kg^{-1}	[22]
Density, ρ	1200	kg m^{-3}	[22]
Crystallization heat, ΔH_c	38300	J kg^{-1}	[15]
Convection coefficient, h	1572–1560	J m^{-2} K^{-1} s^{-1}	
Equilibrium melting temperature, T_m^0	169.9	°C	[22]
Glass transition temperature, T_g	0	°C	
Initial temperature, T_0	187	°C	
Activation energy, kinetic crystallization, E_{a_1,T_m} E_{a_2,T_g}	2807 2696	J mol^{-1} J mol^{-1}	[16]
Kinetic exponent, n	2		[16]
Pre-exponential constant, k_0	$9.142 \cdot 10^{-2}$	s^{-n}	[16]
Activation energy, isothermal induction time E_{i_1,T_m} E_{i_2,T_g}	5760 1790	J mol^{-1} J mol^{-1}	[22]
Pre-exponential, isothermal induction time, k_{i_0}	$9.5 \cdot 10^{-4}$	s	[22]

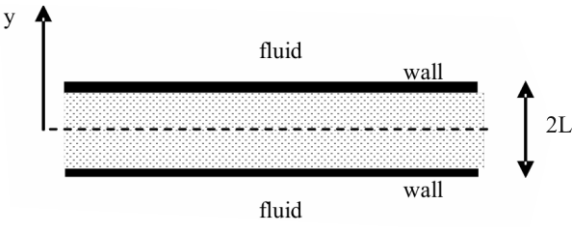

Fig. 1 Configuration of the mold used for the simulation

The one-dimensional unsteady-state heat transfer rate through the sheet thickness is given by the following thermal energy equation:

$$\rho C_p \frac{\partial T}{\partial t} = \kappa \frac{\partial T^2}{\partial y^2} + \rho(-\Delta H_c)\frac{dX_r}{dt} \quad (5)$$

This equation relates the relative crystallinity (X_r) and absolute temperature (T), as a function of time (t) and the position in the sheet thickness (y) for given values of crystallization heat (ΔH_c), thermal conductivity (κ), density (ρ) and specific heat (C_p) [23]. Equation (5) can be written as:

$$\frac{\partial T}{\partial t} = \alpha \frac{\partial^2 T}{\partial y^2} + \frac{-\Delta H_c}{C_p}\frac{dX_r}{dt} \quad (6)$$

where $\alpha=\kappa/\rho C_p$ is the thermal diffusivity.

The dimensionless form of the Eq. (6) is:

$$\frac{\partial \theta}{\partial \lambda} = \frac{\partial^2 \theta}{\partial \xi^2} + \beta \frac{dX_r}{d\lambda} \quad (7)$$

where

$$\theta=T/T_0 \quad \lambda==t\alpha/L^2 \quad \xi=y/L \quad \beta=-\Delta H_c/C_p T_0 \quad (8)$$

The first term on the right-hand side in Eq. (7) represents the heat transfer due to conduction and the second represents the heat source associated with the heat generated during crystallization (Eq. (2)).

For cooling with a chilling fluid applied to the wall sheet, the initial conditions are:

$$T=T_0,\ X_r=0 \text{ at } t=0\ \forall y \quad (9)$$

The boundary conditions are the following:

$$y=0 \qquad dT/dy=0 \quad (10)$$

$$y=L \qquad \kappa\frac{dT}{dy} = h(T_{wall} - T_{water}) \quad (11)$$

where κ is PHBV thermal conductivity, h is the convection coefficient, T_{wall} is the temperature of the wall, T_{water} is the remote temperature of the water used as cooling fluid, $2L$ is the sheet thickness and y is the position in the thickness. Water convection coefficient values were obtained applying the analogy of Reynolds modified by Von Karman [24] and are valid in the temperature range between 20 and 80°C. The flow rate considered was 0.5 m s^{-1}, parallel to the horizontal plain of the sheet.

Temperature, crystallization rate and relative crystallinity profiles developed during cooling under a constant temperature of the chilling fluid and for different thicknesses, were calculated from the temperature and crystallinity variation with time (Eq. (6)) coupled to the non-isothermal crystallization model [Eqs (2)–(5)]. An implicit finite-difference method (Crank–Nicholson scheme) was used to solve the thermal energy equation. The dX_r/dt in the heat source term of Eq. (6) was evaluated by using an explicit

method. The sample thickness was divided into 100 evenly spaced nodes between the centerline and the wall (Fig. 1). The time step at which the system was solved was less than 0.003 s.

Results and discussion

The most desired cooling conditions are those which provide uniform temperature across the thickness in a short molding time [13]. Temperature profiles within the part may lead to crystallinity and morphology profiles which in turn lead to undesirable variations in the mechanical properties. Generally, morphology distribution throughout the part thickness upon cooling in a mould mainly depends on the combination of two factors: the coolant fluid temperature and the thickness considered. Therefore, the model was used to analyze the effect of these two parameters on the temperature, crystallization rate (dX_r/dt) and X_r unsteady-state profiles generated during the solidification stage.

Firstly, the simulation of the crystallization upon cooling requires of the knowledge of a continuous function that relates the kinetic constant k with the temperature, T. Isothermal calorimetric experiment allow one to obtain only a limited number of experimental data restricted by the boundary temperatures (cold crystallization and melt crystallization). Experimental kinetic parameters obtained in isothermal experiments performed at different temperatures [16] were used to verify the ability of Eq. (2) to describe the dependence of the kinetic constant over a broad range of temperatures. Equation (2) represents correctly the dependence of the kinetic constant with temperature because it shows a bell-shape between T_g and T_m, being zero at these two temperatures [20]. Figure 2 represents the results of applying Eq. (2). A good agreement between experimental data and theoretical results was found, indicating the ability of the simplest Eq. (2) to represent the temperature dependence of the kinetic constant for PHBV. Theoretically, the greatest crystallization rate would occur at about 80°C. This value agrees well with that proposed by El-Hadi *et al.* [7] as the ideal crystallization temperature for PHB and its blends.

In order to analyze the solidification step under cooling conditions comparable with that currently using in industrial processing, different water temperatures (cooling fluid) varying from 20 to 80°C were selected. Predicted temperature profiles for two specific positions, the wall and the center, generated under different constant cooling fluid temperatures for a 20 mm-thick part are depicted in Fig. 3. The slope of the temperature curves represents the local cooling rate for each position within the part. Temperature decreases from the wall to the center creating a surface-to-center differentiation which may impact on the morphology distribution. Particularly, at the inner part three steps can be distinguished in the temperature curve. Initially the part is cooling from the molten state well before the beginning of the crystallization process. In this stage the temperature profiles respond to Fourier´s law under non-steady conditions, which is a function of the conductivity of the melt, the thickness of the part and the boundary conditions imposed. During the second step the temperature profiles generated are the result of two competing factors: (a) the rate of heat generated by the exothermic crystallization rate and (b) the conductive flux toward the walls. The exothermic crystallization reaction produces a significant decrease in the local cooling rate, became more significant in the center of the piece. As expected this effect becomes more significant as the thickness or fluid temperature increase [13, 14]. After complete crystallization occurred, the temperature profiles were controlled only by Fourier´s law. It is clear, that temperature profiles for each fluid temperature and part thickness were slightly different and will determine the most suitable cooling conditions to obtain even crystallinity profiles across the part thickness.

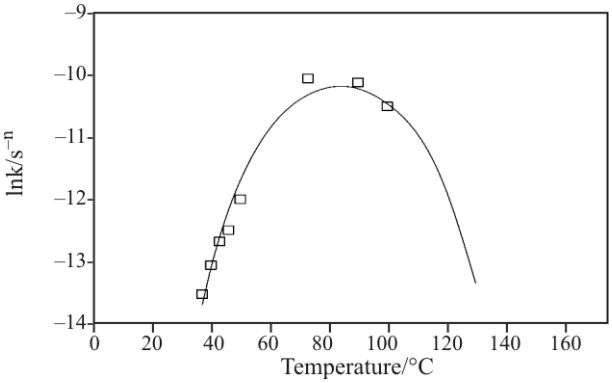

Fig. 2 Comparison between kinetic constants evaluated from isothermal calorimetric experiments [16] and Eq. (2)

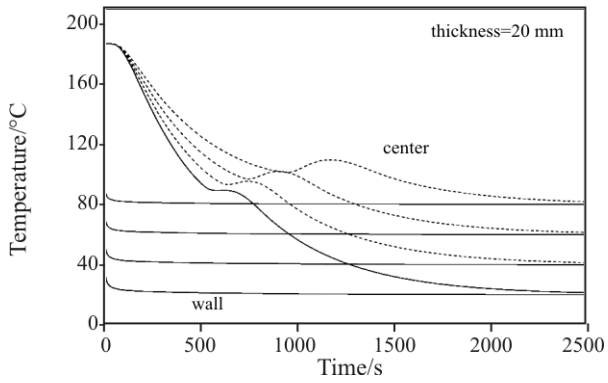

Fig. 3 Effect of different constant fluid temperatures on the temperature profiles at the center of a 20 mm-thick part

The simulation was used to predict the effect of different constant fluid temperatures (20, 40, 60 and 80°C) on the temperature and crystallization rate profiles at the wall and center of a PHBV part. The total time was determined as that taken for the first slice (or node) of polymer melt to reach X_r=1. The onset, maximum and end of the crystallization process for these two extreme positions at a given fluid temperature are collected in Table 2.

Figure 4a shows the predicted temperature profiles and crystallization rate across the thickness of a 10 mm thick part cooled at a constant fluid temperature of 20°C. Temperature profiles do not show any increment even at the center due to the fact that the conduction term prevails over the crystallization heat released. Therefore, the center attains only an X_r of about 0.15 (Table 2). On the other hand, crystallization at the wall takes 30000 s to start. The onset and overall crystallization process at the wall are governing by the first exponential in [Eqs (2) and (3)]. For a cooling temperature near T_g the molecular motion in the amorphous phase is restricted and prevents further crystallization. Thus, cooling a thick part at 20°C will produce well defined temperature profiles from the surface to the center which in turn may lead to a distribution of the relative crystallinity. By increasing the part thickness up to 20 mm (Fig. 4b) the inner part starts to crystallize at 530 s and the complete process takes 1043 s. The simulation predicted almost complete crystallization across the thickness, except for the wall.

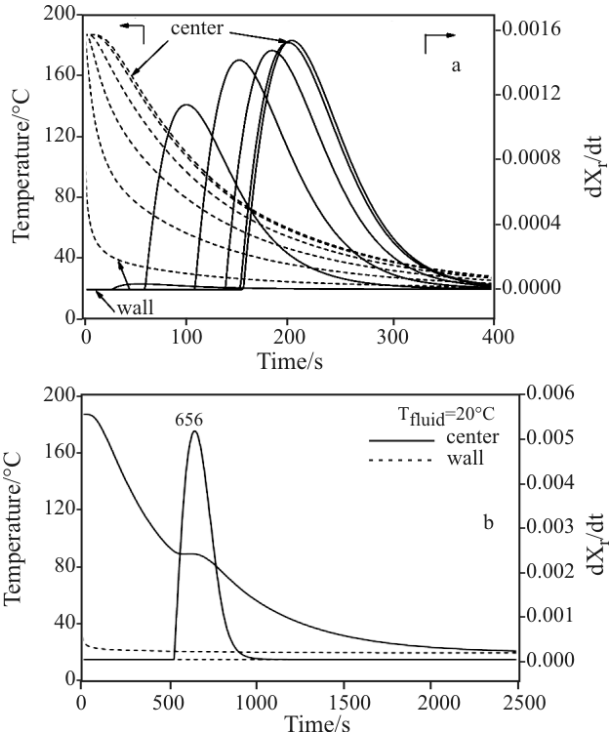

Fig. 4 Temperature and crystallization rate profiles for two different thicknesses. a – 10, b – 20 mm

By increasing the fluid temperature, more uniform crystallinity distribution is expected. Figure 5a represents the predicted crystallization rate profiles for a constant fluid temperature of 40°C. Crystalliza-

Table 2 Time for the onset, maximum and end of the crystallization process at the wall and at the center for three different PHBV part-thicknesses cooled at different constant water temperature

Thickness/mm	Wall			Center		
	Onset time/s	Peak time/s	Final time/s	Onset time/s	Peak time/s	Final time/s
Fluid temperature 20°C						
10	3088	–	–	155	204	1500 (X_r=0.15)
20	2403	–	–	537	656	1043 (X_r=1)
30	2064	–	–	1136	1271	1607 (X_r=1)
40°C						
10	28	433	1498	183	287	1408
20	28	435	1498	572	736	1035
30	28	485	1498	1319	1453	1812
60°C						
10	20	174	576	214	338	693
20	20	172	574	750	879	1197
30	20	172	574	1553	1710	2106
80°C						
20	35	153	530	965	1091	1541

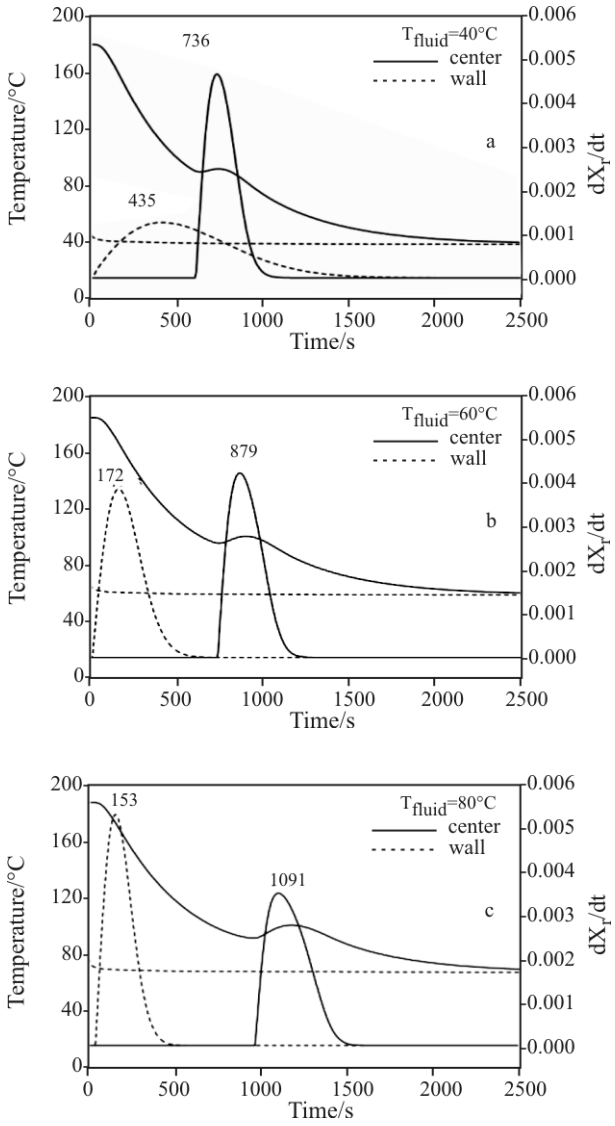

Fig. 5 Temperature and crystallization rate profiles generated at the wall (dot line) and center (solid line) of a 20 mm-thick part of PHBV cooled under different constant fluid temperatures. a – 40, b – 60 and c – 80°C

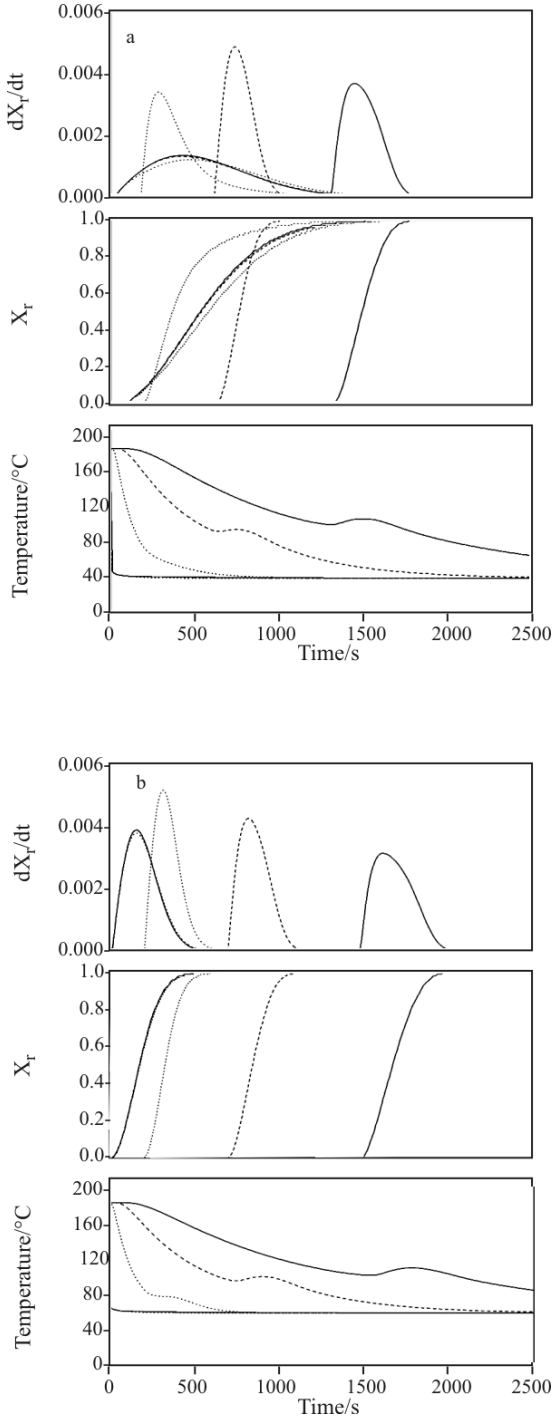

Fig. 6 Temperature, relative crystallinity and crystallization rate profiles developed at the wall and center for parts with thickness of 10 mm (solid line), 20 mm (dash line) 30 mm (dot line) at two constant fluid temperatures. a – 40 mm, b – 60°C

tion at the wall begins as soon as the cooling process starts and takes 1600 s to complete the process, whereas at the center the onset of crystallization is found around 600 s and complete crystallization is achieved in 1100 s. It is important to note that the crystallization rate at the wall is slower than that at the center due to the restrictions imposed near T_g. This effect is similar to that above discussed for a fluid temperature of 20°C but it is less dramatic because of the higher fluid temperature used. As expected, the restrictions due to T_g became less significant as the fluid temperature increases as can be seen from the predicted profiles obtained at a constant fluid temperature of 60°C (Fig. 5b). Crystallization at the wall takes 574 s meanwhile at the center the process finishes at 1200 s and at similar crystallization rates. On the other hand, for a fluid temperature of 80°C (Fig. 5c), crystallization at the wall starts at 28 and takes 410 s to complete the process, whereas at the core region the onset of crystallization is predicted at 960 s and longer time than for 60°C is needed to com-

plete the process. For this fluid temperature, the second exponential in Eqs (2) and (3) become more important and the onset and overall crystallization are controlled by the degree of undercooling. As a consequence of these results, whatever the fluid temperature, the model predicts surface-to-center differentiation. However, by selecting 40 and 60°C as fluid temperature this effect can be minimized and almost uniform crystallinity profiles may be achieved in a reasonable time. As a consequence, these two temperatures were chosen as the more suitable cooling conditions and were used to predict their effect on morphology profiles for different part thicknesses and the results are summarized in Figs 6a and b. For a given fluid temperature, the increment in the local temperature in the center of the part increases with the thickness. This result suggests that the influence of the crystallization heat become major with the thickness increment. The time of the overall crystallization process also increased with thickness (Table 2) because the increment in the local temperature slowed the crystallization rate. By cooling at 40°C, the model predicted even relative crystallinity profiles for 10 and 20 mm-thick parts (Fig. 6a) while for larger thicknesses (i.e. 30 mm) the center took longer time to reach complete crystallinity due to higher increment in the local temperature (which slows the crystallization rate). When a constant fluid temperature of 60°C is used, the wall and center reach even crystallinity profiles within a 10 mm-thick part. Under this condition and for higher thicknesses (i.e. 20 and 30 mm) the model predicts well defined surface-to-center crystallinity profiles (Fig. 6b). As a conclusion, by selecting the appropriate fluid temperature for a given part thickness, uniform relative crystallinity profiles may be attained in a reasonable time scale, i.e. by cooling a 10 mm-thick part with a constant fluid temperature of 60°C uniform relative crystallinity profiles can be obtained. For thicknesses higher than 20 mm, the decrease in the crystallization rate at the core region seems to be inevitable and uneven crystallinity profiles are predicted.

Conclusions

The numerical simulation proposed in this work was able to predict temperature profiles, relative crystallinity and crystallization rate profiles developed during the cooling stage of a PHBV part using water as the chilling fluid. The numerical approach proposed has the ability of predicting, in a single step, the optimal conditions to obtain uniform relative crystallinity throughout the part thickness by varying the fluid temperature and the part thickness.

Fluid temperatures are restricted mainly by T_g and T_m values of the material (Table 1) which define the processing window of PHBV. The predicted maximum crystallization rate was found for a temperature around 80°C. Thus, by applying a fluid at such temperature even crystallinity profiles should be expected. However, the model predicted surface-to-center temperature and crystallinity profiles.

The model predicts a crystallization temperature window in the range of $20<T<60$°C. The T_g value (T_g=0°C) limiting the application of fluid temperatures lower than 20°C whereas cooling temperatures higher than 60°C resulted in higher overall crystallization time. For temperatures between these two boundary values, the optimal processing conditions depend on the combination of two variables: the fluid temperature and the thickness considered. For PHBV pieces with thicknesses lower or equal than 10 mm, even crystallinity profiles may be obtained by cooling the part at a constant fluid temperature of 60°C, meanwhile for thicknesses up to 20 mm 40°C was found to be the more appropriate condition.

Acknowledgements

We thank ANPCYT, contract grant number: PICT 12-1560, and National Research Council, Argentina (CONICET), contract grant number PIP6258/05 for their financial support.

References

1 S. Khanna and A. K. Srivastava. Process. Biochem., 34 (2005) 607.
2 Y. Doi, Microbial Polyesters, VCH, New York 1990.
3 M. Avella, E. Martuscelli and M. Raimo, J. Mater. Sci., 35 (2000) 523.
4 V. P. Cyras, A. Vázquez, Ch. Rozsa, N. Galego, L. Torre and J. M. Kenny, J. Appl. Polym. Sci., 77 (2000) 2889.
5 N. Galego, Ch. Rozsa, R. Sánchez, J. Fung, A. Vázquez and J. Santo Tomás, Polym. Test., 19 (2000) 485.
6 E. Withey and J. N. Hay, Polymer, 40 (1999) 5147.
7 A. El-Hadi, R. Schnabel, E. Straube, G. Müller and M. Reimscheide, Macromol. Mater. Eng., 287 (2002) 363.
8 G. R. Saad and H. Sliger, Polym. Degrad. Stab., 83 (2004) 101.
9 A. El-Hadi, R. Schnabel, E. Straube, G. Müller and S. Henning, Polym. Test., 21 (2002) 665.
10 L. M. W. K. Gunaratne and R. A. Shanks, J. Therm. Anal. Cal., 83 (2006) 313.
11 R. M. Patel and J. E. Spruiell, Polym. Eng. Sci., 31(1991)730.
12 N. Sombatsompop and A. Tangsongcharoen, J. Appl. Polym. Sci., 82 (2001) 2087.
13 R. A. Ruseckaite, P. M. Stefani, V. P. Cyras, J. M. Kenny and A. Vázquez, J. Appl. Polym. Sci., 82 (2001) 3275.
14 V. P. Cyras, P. M. Stefani, R. A. Ruseckaite and A. Vázquez, Polym. Compos., 25 (2004) 461.

15 J. K. Deporter and D. G. Baird, Polym. Compos., 17 (1996) 210.
16 Ch. Rozsa , P. Ortz., V. P. Cyras, A. Vázquez and N. Galego, Intern. J. Polym. Mater., 51 (2002) 619.
17 B. Wunderlich, Macromolecular Physics, Vol. 2, Academic Press, New York 1977.
18 M. R. Kamal and E. Chu, Polym. Eng. Sci., 23 (1983) 27.
19 C. C. Lin, Polym. Eng. Sci., 23 (1983) 113.
20 L. Torre, A. Maffezzoli and J. M. Kenny, J. Appl. Polym. Sci., 56 (1995) 985.
21 V. A. Alvarez, P. M. Stefani and A. Vazquez, J. Therm. Anal. Cal., 79 (2005) 187.
22 V. P. Cyras, Ch. Rozsa Ch., N. Galego and A. Vázquez, J. Appl. Polym. Sci., 94 (2004) 1657.
23 Technical data from the supplier, Aldrich Chemical Co. (Milwaukee, WI).
24 M. Necati Özişik, Heat Conduction, Wiley Interscience Pub., J. Wiley & Sons, Inc., New York 1993.

Received: May 3, 2008
Accepted: September 17, 2008

DOI: 10.1007/s10973-008-8550-0